

## ULTRAFAST OPTICS

# Ultrafast electro-optic light with subcycle control

David R. Carlson<sup>1\*</sup>, Daniel D. Hickstein<sup>1†</sup>, Wei Zhang<sup>1</sup>, Andrew J. Metcalf<sup>1</sup>, Franklyn Quinlan<sup>1</sup>, Scott A. Diddams<sup>1,2</sup>, Scott B. Papp<sup>1,2\*</sup>

Light sources that are ultrafast and ultrastable enable applications like timing with subfemtosecond precision and control of quantum and classical systems. Mode-locked lasers have often given access to this regime, by using their high pulse energies. We demonstrate an adaptable method for ultrastable control of low-energy femtosecond pulses based on common electro-optic modulation of a continuous-wave laser light source. We show that we can obtain 100-picojoule pulse trains at rates up to 30 gigahertz and demonstrate sub-optical cycle timing precision and useful output spectra spanning the near infrared. Our source enters the few-cycle ultrafast regime without mode locking, and its high speed provides access to nonlinear measurements and rapid transients.

Ultrafast lasers produce trains of femtosecond-duration light pulses and can operate as frequency combs to provide a time and frequency reference bridging the optical and microwave domains of the electromagnetic spectrum (1). Achieving phase control of these pulse trains to better than a single optical cycle has enabled diverse applications ranging from optical atomic clocks (2) to controlling quantum states of matter (3, 4). These capabilities have evolved over decades, and yet they still require the intrinsic stability of a suitable mode-locked resonator.

One alternative method that produces optical pulse trains without mode locking is electro-optic modulation (EOM) of a laser (5, 6). These pulse generators, or “EOM combs,” first gained interest nearly 50 years ago because of their simplicity, tunability, reliability, commercialization, and spectral flatness (7–10). Nevertheless, despite their broad appeal and decades of development, the fundamental goal of electronic switching with the optical-cycle precision needed to create ultrafast trains of EOM pulses has remained unmet, limited by thermodynamic noise and oscillator phase noise inherent in electronics.

Here, we report the generation of ultrafast and ultrastable electro-optic pulses without any mode locking. Our experiments demonstrate widely applicable techniques to mitigate electro-optic noise by relying on the quantum-limited optical processes of cavity transmission, nonlinear interferometry, and nonlinear optical pulse compression, as well as low-loss microwave interferometry. This results in phase control of ultrafast electro-optic fields with a temporal precision better than one cycle of the optical carrier. Because electro-

optic sources support pulse repetition rates greater than 10 GHz, our work opens up the regime of high-speed, ultrafast light sources, enabling sampling or excitation of high-speed transient events, as well as making precision measurements across octaves of bandwidth.

We demonstrate the performance of our ultrafast phase control by directly carving electro-optic pulse trains at 10 and 30 GHz with ~1-ps initial pulse durations and show that these pulses can be spectrally broadened to octave bandwidths and temporally compressed to less than three optical cycles (15 fs) in nanophotonic silicon-nitride (Si<sub>3</sub>N<sub>4</sub>, henceforth SiN) waveguides. To deliver a femtosecond source timed with subcycle precision, we introduce an EOM-comb configuration implementing high-Q microwave-cavity stabilization of the 10-GHz electronic oscillator. This oscillator is phase-locked to the continuous-wave (CW) pump source via  $f - 2f$  stabilization of the carrier-envelope offset, enabling complete knowledge of the ~28,000 EOM-comb frequencies to 17 digits. Our implementation uses a cavity-stabilized CW laser to demonstrate subhertz-linewidth modes spanning the near infrared, but we note that more standard pump sources could achieve the same relative stability between the microwave source and optical carrier.

Our EOM comb is derived from a microwave source that drives an intensity modulator placed in series with multiple phase modulators to produce a 50%-duty-cycle pulse train with mostly linear frequency chirp (Fig. 1). In the spectral domain, this process results in a deterministic cascade of sidebands with prescribed amplitude and phase that converts the CW laser power into a frequency comb with a mode spacing given by the microwave driving frequency  $f_{\text{eo}}$ . The frequency of each resulting mode  $n$ , counted from the CW laser at frequency  $\nu_p$ , can then be expressed as  $\nu_n = \nu_p \pm n f_{\text{eo}}$ . Equivalently, the modes can be expressed as a function of the classic offset frequency  $f_0$  and repetition rate  $f_{\text{rep}}$  parameters as  $\nu_n = f_0 + n f_{\text{rep}}$ , where now the mode number  $n'$  is counted from zero frequency and  $f_{\text{rep}} = f_{\text{eo}}$ .

In order for the EOM comb to achieve ultra-stable coherence between  $\nu_p$  and  $f_{\text{eo}}$ , it is vital to keep the integrated phase noise of each mode below  $\pi$  radians. In the temporal domain, this corresponds to subcycle timing jitter, and for EOM combs this requirement becomes more difficult to achieve as the comb bandwidth is increased because of microwave-noise multiplication (11). For octave-spanning spectra at a 10-GHz repetition rate, this multiplication factor is  $n' \approx 20,000$  and corresponds to an 86-dB increase in phase noise. Thus, reaching the  $\pi$ -radian threshold with an EOM comb requires careful treatment of the noise at all Fourier frequencies.

As noted earlier (10), broadband thermal noise in the electronic components up to the Nyquist frequency causes the phase-coherence threshold to be exceeded. To compensate, a Fabry-Pérot cavity optically filters the broadband thermal noise fundamental to electro-optic modulation, resulting in a detectable carrier-envelope offset frequency. However, the cavity linewidth (typically a few megahertz) places a lower bound on the range of frequencies where this suppression is possible, and therefore, it is additionally necessary to investigate the use of low-noise microwave oscillators. This is especially important for the Fourier-frequency range between 100 kHz and the filter-cavity linewidth, where high-gain feedback is technically challenging.

In the stabilized EOM comb (a comprehensive system diagram is shown in fig. S1), we use a commercial dielectric-resonator oscillator (DRO) with a nominal operating frequency of 10 GHz and 0.1% tuning range to drive the modulators. Compared to other commercial microwave sources, the DRO offers improved phase-noise performance in the critical Fourier-frequency range between 100 kHz and 10 MHz. The DRO output is then amplified before driving the phase modulators to produce the typical comb spectrum shown in Fig. 2A.

After transmission through an optical-filter cavity to suppress thermal noise, the chirped-pulse output of the EOM comb is compressible to durations as short as 600 fs, depending on the initial spectral bandwidth. Unfortunately, pulse durations greater than ~200 fs pose problems for coherent supercontinuum broadening in nonlinear media with anomalous dispersion (12, 13). However, if the nonlinear material instead exhibits normal dispersion, broadening due to pure self-phase modulation is known to produce lower-noise spectra owing to the suppression of modulation instability (13). Consequently, we employ a two-stage broadening scheme using a normal-dispersion highly nonlinear fiber (HNLF) to achieve initial spectral broadening (14–16) and pulse compression to 100 fs (17), followed by an anomalous-dispersion SiN waveguide for broad spectrum generation.

High-repetition rate lasers ( $f_{\text{rep}} \geq 10$  GHz) produce lower pulse energies for the same average power, making it challenging to use nonlinear broadening to produce the octave bandwidths required for self-referencing. However, patterned nanophotonic waveguides have recently emerged

<sup>1</sup>Time and Frequency Division, National Institute of Standards and Technology, 325 Broadway, Boulder, CO 80305, USA.

<sup>2</sup>Department of Physics, University of Colorado, 2000 Colorado Avenue, Boulder, CO 80309, USA.

\*Corresponding author. Email: david.carlson@nist.gov; scott.papp@nist.gov

<sup>†</sup>Present address: KMLabs, Inc., 4775 Walnut Street, Suite 102, Boulder, CO 80301, USA.

as a promising platform owing, in part, to their high nonlinearity and engineerable dispersion (18–20). Here, we demonstrate input-coupling efficiency to a SiN waveguide of up to 85% (17) that enables a broadband supercontinuum to be generated with pulses from high-repetition rate ultrafast sources. The spectra generated with our 10-GHz EOM comb spans wavelengths from 750 nm to beyond 2700 nm for two different waveguide geometries (Fig. 2B), producing a total integrated power of ~1.1 W. Individual comb lines across the entire bandwidth exhibit a high degree of extinction (50 dB at 1064 nm; see fig. S2 for data at 775, 1064, and 1319 nm) and do not exhibit any intermode artifacts such as sidebands, a common problem when mode filtering is used to convert low-repetition rate combs to high repetition rates (21).

To investigate the scalability to even higher repetition rates, we made additional supercontinuum measurements using a 30-GHz EOM comb, which produced 600-fs, 70-pJ pulses (Fig. 2D). Despite the three-times reduction in pulse energy compared to the 10-GHz comb, similar broadband spectra are readily obtained. In both cases, if the waveguide input pulse energy is kept below ~100 pJ, smooth spectra can be obtained with high power per comb mode.

For applications requiring very flat spectra over broad bandwidths, such as astronomical spectrograph calibration (22), the supercontinuum

light can be easily collected in a single-mode fiber and flattened with a single passive optical attenuator. Under these conditions, fluctuations in spectral intensity can be kept within  $\pm 3$  dB over wavelengths spanning from 850 to 1450 nm while delivering more than 10 nW per mode in the fiber at 10 GHz. Improved waveguide-to-fiber output coupling, or free-space collimation combined with an appropriate color filter, could further improve the power per mode.

After broadening in the SiN waveguide, the offset frequency is detected with >30 dB signal-to-noise ratio (SNR), suggesting that the scheme of combining normal- and anomalous-dispersion media indeed allows us to overcome the difficulties of producing a coherent supercontinuum using pulses longer than a few hundred femtoseconds; see fig. S3 for SNR versus bandwidth. Stabilization of  $f_0$  is subsequently accomplished by feeding back to the frequency-tuning port of the DRO. However, owing to optical and electronic phase delay in this configuration, the feedback bandwidth is limited to ~200 kHz (Fig. 3A, blue curve) and thus is insufficient on its own to narrow the comb linewidth set by the multiplied microwave noise of the DRO.

To reach the  $\pi$ -radian threshold for phase coherence between the CW laser and electronic oscillator, the output of one high-power microwave amplifier is stabilized to an air-filled aluminum

microwave cavity in the stabilized-local-oscillator (STALO) configuration (23, 24) and yields an immediate reduction in phase noise of up to 20 dB at frequencies less than 500 kHz from the carrier.

In Fig. 3A, we use the  $\beta$ -line (25) to distinguish between regimes where the linewidth of the comb offset  $f_0$  is adversely affected (phase noise above the  $\beta$ -line) and where there is no linewidth contribution (phase noise below the  $\beta$ -line). Having phase noise below the  $\beta$ -line at all points is approximately equivalent to an integrated phase noise below  $\pi$  radians, and thus provides a convenient visual way to assess the impact of noise at different Fourier frequencies. For our EOM comb, the  $f_0$  phase noise remains below the  $\beta$ -line at all frequencies only when both the STALO lock and the  $f - 2f$  lock are used in tandem. Under these conditions, noise arising from the microwave oscillator does not contribute appreciably to the comb linewidth and thus, the CW laser stability is faithfully transferred across the entire comb bandwidth. Equivalently, integrating the phase noise of the fully locked  $f_0$  beat (1.17 rad, 10 Hz to 4 MHz) yields a pulse-to-pulse timing jitter of 0.97 fs (1.9 fs if limited by the  $\beta$  line between 4 MHz and 5 GHz) (17), indicating that the microwave envelope coherently tracks the optical carrier signal with subcycle precision.

The progression of offset-frequency stabilization is also shown by the beat frequencies as each

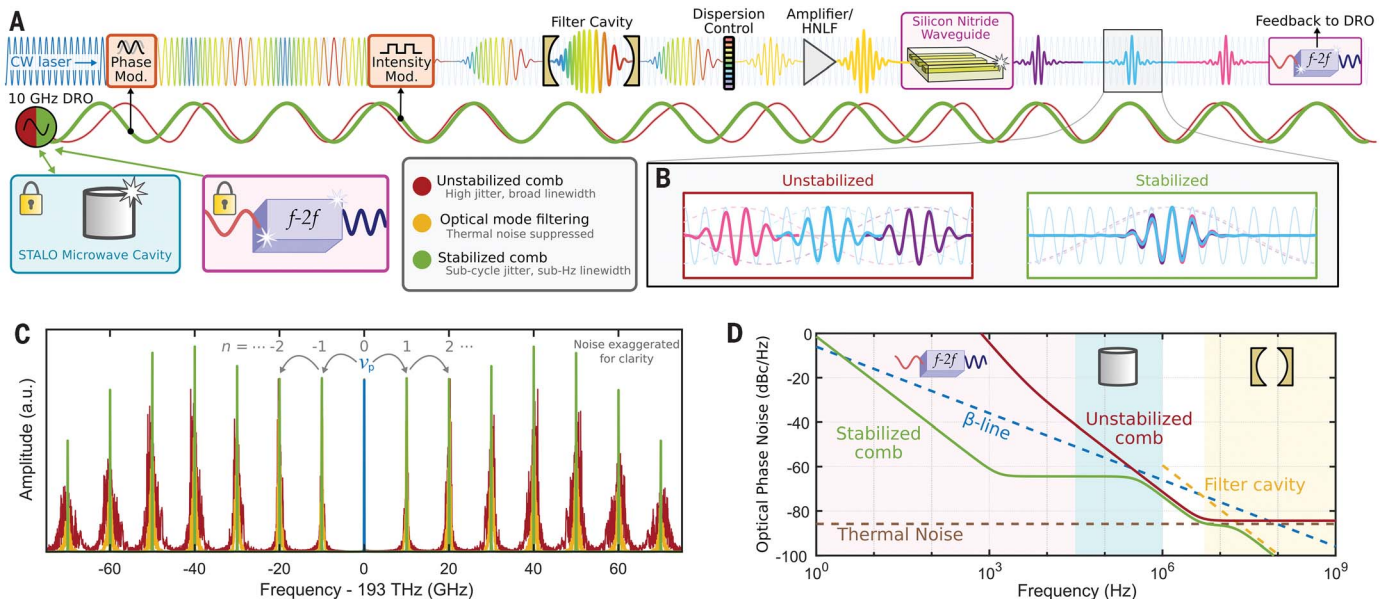


**Fig. 1. Carving femtosecond pulses from a continuous-wave (CW) laser with subcycle precision.** (A) A chirped pulse train is derived from a 1550-nm CW laser by electro-optic phase and intensity modulation driven by a 10-GHz dielectric resonant oscillator (DRO) that is locked to a high-Q microwave cavity in the stabilized-local-oscillator (STALO) configuration. The pulse train is then optically filtered by a Fabry-Pérot cavity to suppress electronic thermal noise on the comb lines before spectral broadening in highly nonlinear fiber (HNLF) followed by a silicon-nitride waveguide. Octave-spanning spectra allow detection of the comb offset frequency in an  $f - 2f$  interferometer that is used to stabilize the DRO output. (B) Without stabilization, the microwave-derived pulse train exhibits large pulse-to-pulse timing jitter relative

to the CW carrier. When the drive frequency is stabilized by feedback from the comb offset frequency and the STALO cavity, sub-optical cycle phase coherence between successive pulses is achieved. Note that the stabilized pulses are shown with zero carrier-envelope offset, though this is not generally the case. (C) In the frequency-domain picture, the unstabilized comb (red) exhibits large noise multiplication as the mode number  $n$  expands about zero. Mode filtering (yellow) suppresses high-frequency thermal noise. The fully stabilized comb lines (green) appear as  $\delta$ -functions because the CW-laser stability is transferred across the entire comb bandwidth. (D) Optical phase noise picture of the comb, showing the effects of the  $f - 2f$  stabilization, STALO cavity, and filter cavity.

lock is turned on (Figs. 3, B to D). The coherent carrier seen in the offset frequency when fully stabilized (Fig. 3D) indicates that phase coherence has been achieved between individual comb lines across the entire available spectral bandwidth. The accuracy and precision of the stabilized EOM comb were determined by beating the 10-GHz repetition rate against the 40th har-

monic of an independent mode-locked laser operating at 250 MHz (17). After 2000 s of averaging, a fractional stability of  $3 \times 10^{-17}$  was obtained with no statistically significant frequency offset observed. This level of accuracy represents an improvement of more than three orders of magnitude over previously demonstrated EOM-comb systems (10) and is likely only limited here by

averaging time and out-of-loop path differences between the two combs.

To further show the versatility of the EOM comb as an ultrafast source, we describe how to create pulses that have durations lasting only a few cycles of the optical field. Pulses in this regime can provide direct access to the carrier-envelope phase and high peak intensities but require a well-controlled output spectrum exhibiting a high degree of spectral flatness and coherence. However, achieving such pulses at gigahertz repetition rates with mode-locked lasers is technically challenging. Still, high-repetition rate sources of few-cycle pulses could be valuable for applications like optically controlled electronics (26, 27), where both fast switching speeds and peak intensity are important. Similarly, coherent Raman imaging of biological samples can benefit from transform-limited ultrashort pulses (28), but the acquisition speed for broadband spectra is typically restricted by the megahertz-rate mode-locked laser sources that are used. Extending to higher repetition rates could reduce measurement dead time and also prevent sample damage due to high peak powers (29).

The use of optical modulators to directly carve a train of ~1-ps pulses from a CW laser provides an effective method for generating clean few-cycle pulses thanks to the soliton self-compression effect (30, 31). To achieve this, the pulse power and chirp incident on the SiN waveguide are adjusted such that the launched pulse approaches the threshold peak intensity for soliton fission near the output facet of the chip. A normal-dispersion single-element aspheric lens is then used to out-couple the light without introducing appreciable higher-order dispersion, and a 2-cm-long rod of fused silica recompresses the pulse to near its transform limit. Figure 4 shows the reconstructed pulse profile obtained through frequency-resolved optical gating (FROG) (32). Pulse durations of 15 fs (2.8 optical cycles, full width at half maximum) and out-coupled pulse energies in excess of 100 pJ (1 W average power) are readily achievable at a repetition rate of 10 GHz.

The combination of high-repetition rate pulse trains, ultrastable broadband frequency synthesis, few-cycle pulse generation, and extensible construction in our EOM-comb system provides a versatile ultrafast source with other additional practical benefits. For instance, these combs could also support further photonic integration through complementary metal-oxide-semiconductor (CMOS)-compatible modulators (33), alignment-free construction, the use of commercially sourceable components, and straightforward user customization. Moreover, whereas the optical and microwave cavities currently limit the broad tuning capability of the repetition rate, the ~300 THz of comb bandwidth places a mode within 5 GHz of any spectral location in this range. By overcoming several experimental challenges related to broadening and stabilizing noisy picosecond-duration pulses, our techniques are widely applicable to existing technologies with demanding requirements, such as chip-based microresonators (34) or semiconductor lasers (35).

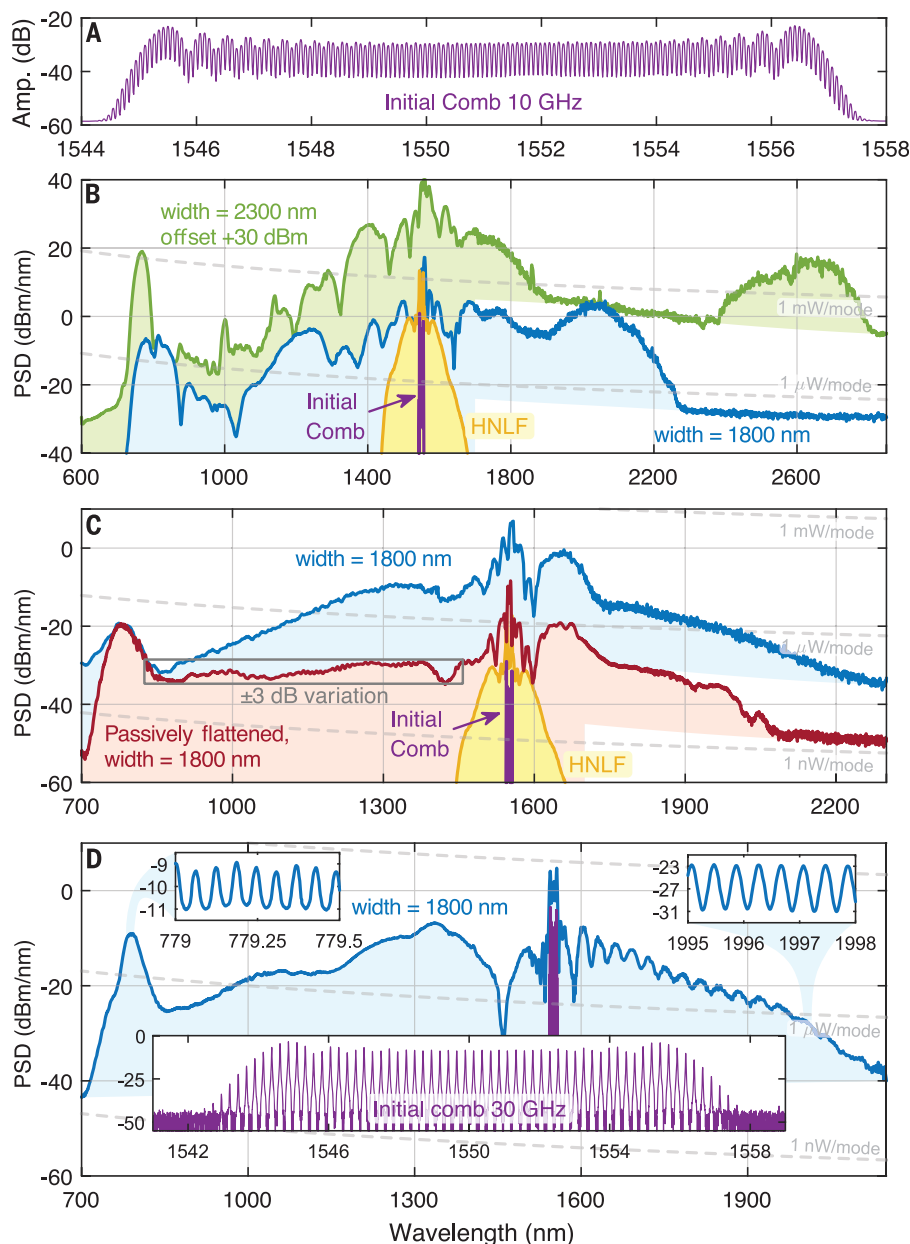


**Fig. 2. High-repetition-rate supercontinuum.** (A) Spectrum of the 10-GHz EOM comb directly after generation. (B) Ten-gigahertz supercontinuum spectra spanning from 750 to 2750 nm for two different silicon-nitride waveguide widths. The spectral intensity is scaled to intrawaveguide levels. Also shown is the spectrum of the first-stage highly nonlinear fiber (HNLF). (C) Ten-gigahertz supercontinuum optimized for spectral smoothness by reducing incident power (blue). Between 830 and 1450 nm, a flat spectrum ( $\pm 3$  dB) is produced by a single passive optical attenuator (red). (D) Supercontinuum spectrum from a 30-GHz EOM comb. Top insets show that comb coherence is maintained across the entire spectrum (optical SNRs are spectrometer limited). Bottom inset shows initial spectrum of the 30-GHz EOM comb. The y axes in both (C) and (D) show the power spectral density (PSD) obtained in the output fiber.

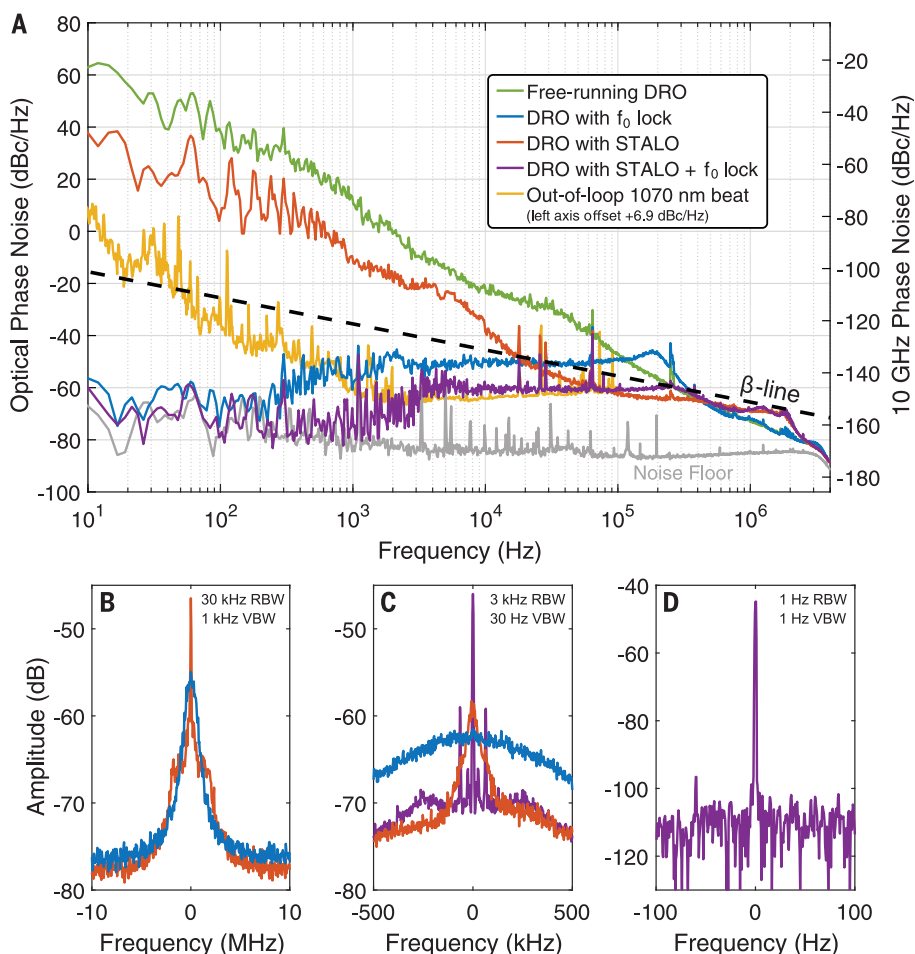


**Fig. 3. EOM-comb phase noise.** (A) Optical phase noise of the comb offset frequency measured at 775 nm (left axis) and scaled to the 10-GHz repetition rate (right axis) under different locking conditions. Prestabilizing the free-running RF oscillator (DRO) using a high-Q microwave cavity in the stabilized-local-oscillator (STALO) configuration lowers the phase noise by up to 20 dB at frequencies below 500 kHz. When servo feedback from the optical  $f_0$  signal is engaged, a tight phase lock is achieved that suppresses low-frequency noise. The  $\beta$ -line indicates the level above which phase noise causes an increase in the comb linewidth. When both the STALO and  $f_0$  locks are engaged, the phase noise remains below the  $\beta$ -line at all frequencies, indicating that the coherence of the CW pump laser is faithfully transferred across the entire comb spectrum. (B to D)  $f_0$  RF beats showing the effects of each feedback loop. A coherent carrier signal is observed (D) only when both the STALO lock and direct  $f_0$  feedback are engaged.

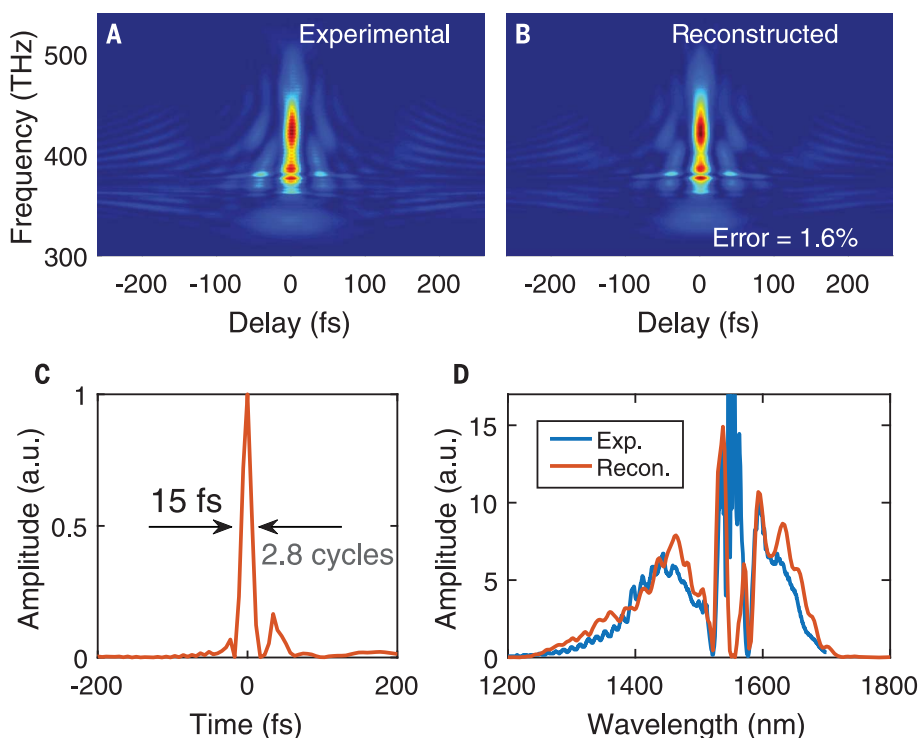


**Fig. 4. Few-cycle pulse generation.** (A) Experimental and (B) reconstructed FROG traces. (C) Reconstructed temporal pulse profile with a full width at half maximum duration of 15 fs (2.8 optical cycles). (D) Comparison of reconstructed and experimental spectra. The quasi-CW spectral wings of the initial comb spectrum near 1550 nm do not contribute appreciably to the pulse and thus are not seen in the reconstructed spectrum. At least 75% of the total optical power is concentrated in the compressed pulse. More sophisticated amplitude and phase compensation of the initial comb spectrum could allow an even larger fraction of the power to be compressed (36).

## REFERENCES AND NOTES

- S. T. Cundiff, J. Ye, *Rev. Mod. Phys.* **75**, 325–342 (2003).
- A. D. Ludlow, M. M. Boyd, J. Ye, E. Peik, P. Schmidt, *Rev. Mod. Phys.* **87**, 637–701 (2015).
- C. Brif, R. Chakrabarti, H. Rabitz, *New J. Phys.* **12**, 075008 (2010).
- D. S. Jin, J. Ye, *Chem. Rev.* **112**, 4801–4802 (2012).
- T. Kobayashi, T. Sueta, Y. Cho, Y. Matsuo, *Appl. Phys. Lett.* **21**, 341–343 (1972).
- M. Kourogi, K. Nakagawa, M. Ohtsu, *IEEE J. Quantum Electron.* **29**, 2693–2701 (1993).
- V. Torres-Company, A. M. Weiner, *Laser Photonics Rev.* **8**, 368–393 (2014).
- J. Li, X. Yi, H. Lee, S. A. Diddams, K. J. Vahala, *Science* **345**, 309–313 (2014).
- G. Millot *et al.*, *Nat. Photonics* **10**, 27–30 (2015).
- K. Beha *et al.*, *Optica* **4**, 406 (2017).
- F. L. Walls, A. DeMarchi, *IEEE Trans. Instrum. Meas.* **24**, 210–217 (1975).
- J. M. Dudley, G. Genty, S. Coen, *Rev. Mod. Phys.* **78**, 1135–1184 (2006).
- K. R. Tamura, H. Kuhota, M. Nakazawa, *IEEE J. Quantum Electron.* **36**, 773–779 (2000).
- C.-B. Huang, S.-G. Park, D. E. Leaird, A. M. Weiner, *Opt. Express* **16**, 2520–2527 (2008).
- R. Wu, V. Torres-Company, D. E. Leaird, A. M. Weiner, *Opt. Express* **21**, 6045–6052 (2013).
- V. Ataie, E. Myslivets, B. P.-P. Kuo, N. Alic, S. Radic, *J. Lightwave Technol.* **32**, 840–846 (2014).
- Supplementary materials are available online.
- A. R. Johnson *et al.*, *Opt. Lett.* **40**, 5117–5120 (2015).
- M. A. G. Porcel *et al.*, *Opt. Express* **25**, 1542–1554 (2017).
- D. R. Carlson *et al.*, *Opt. Lett.* **42**, 2314–2317 (2017).
- D. A. Braje, M. S. Kirchner, S. Osterman, T. Fortier, S. A. Diddams, *Eur. Phys. J. D* **48**, 57–66 (2008).
- T. Steinmetz *et al.*, *Science* **321**, 1335–1337 (2008).
- G. J. Dick, J. Saunders, *IEEE Trans. Ultrason. Ferroelectr. Freq. Control* **37**, 339–346 (1990).
- A. S. Gupta *et al.*, *IEEE Trans. Ultrason. Ferroelectr. Freq. Control* **51**, 1225–1231 (2004).
- G. Di Domenico, S. Schilt, P. Thomann, *Appl. Opt.* **49**, 4801–4807 (2010).
- T. Rybka *et al.*, *Nat. Photonics* **10**, 667–670 (2016).
- C. Karnetzky *et al.*, *Nat. Commun.* **9**, 2471 (2018).
- C. H. Camp Jr., M. T. Cicerone, *Nat. Photonics* **9**, 295–305 (2015).
- K. J. Mohler *et al.*, *Opt. Lett.* **42**, 318–321 (2017).
- G. P. Agrawal, *Nonlinear Fiber Optics* (Academic Press, 2013).
- L. F. Mollenauer, R. H. Stolen, J. P. Gordon, W. J. Tomlinson, *Opt. Lett.* **8**, 289–291 (1983).
- R. Trebino *et al.*, *Rev. Sci. Instrum.* **68**, 3277–3295 (1997).
- G. T. Reed, G. Mashanovich, F. Y. Gardes, D. J. Thomson, *Nat. Photonics* **4**, 518–526 (2010).
- T. Herr *et al.*, *Nat. Photonics* **8**, 145–152 (2013).
- B. W. Tilma *et al.*, *Light Sci. Appl.* **4**, e310 (2015).
- Z. Jiang *et al.*, *IEEE J. Quantum Electron.* **43**, 1163–1174 (2007).

## ACKNOWLEDGMENTS

We thank H. Timmers for assistance making the FROG measurements, A. Hati and C. Nelson for discussions on microwave stabilization, L. Chang for helping lay out the

waveguide lithography masks, K.V. Reddy and S. Patil for discussion of erbium amplifiers, and F. Baynes for constructing the cavity-stabilized laser. **Funding:** This research is supported by the Air Force Office of Scientific Research (AFOSR) under award no. FA9550-16-1-0016, the Defense Advanced Research Projects Agency (DARPA) DODOS program, the National Aeronautics and Space Administration (NASA), the National Institute of Standards and Technology (NIST), and the National Research Council (NRC). This work is a contribution of the U.S. government and is not subject to copyright in the U.S.A. **Author contributions:** The experiment was planned by D.R.C., D.D.H., S.A.D., and S.B.P. The combs were operated by D.R.C. and D.D.H. The optical filter cavity was designed and constructed by W.Z. The 30-GHz measurements were assisted by A.J.M. The data were analyzed by D.R.C., D.D.H., F.Q., S.A.D., and S.B.P. The manuscript was prepared by D.R.C. with input from all coauthors. **Competing interests:** NIST has a pending patent application related to this work. D.H. is currently employed by KMLabs, Inc. **Data and materials availability:** All data are present in the paper or supplementary materials.

## SUPPLEMENTARY MATERIALS

www.sciencemag.org/content/361/6409/1358/suppl/DC1  
Materials and Methods  
Supplementary Text  
Figs. S1 to S5  
References (37–46)

23 April 2018; accepted 1 August 2018  
10.1126/science.aat6451